Characterization of Protonated Formamide-Containing Clusters by Infrared Spectroscopy and Ab Initio Calculations: I. O-Protonation

C.-C. Wu,[†] J. C. Jiang,[‡] I. Hahndorf,[§] C. Chaudhuri,[‡] Y. T. Lee,[†,‡] and H.-C. Chang*[,‡]

Department of Chemistry, National Taiwan University, Taipei, Taiwan 106, R.O.C. and Institute of Atomic and Molecular Sciences, Academia Sinica, P.O. Box 23-166, Taipei, Taiwan 106, R.O.C.

Received: March 15, 2000; In Final Form: June 22, 2000

Characterization of protonated formamide clusters by vibrational predissociation spectroscopy confirms theoretical predictions that O-protonation occurs in preference to N-protonation in formamide. The confirmation is made from a close comparison of the infrared spectra of $H^+[HC(O)NH_2]_3$ and $NH_4^+[HC(O)NH_2]_3$ produced by a supersonic expansion with the spectra produced by ab initio calculations. For $NH_4^+[HC(O)NH_2]_3$, prominent and well-resolved vibrational features are observed at 3436 and 3554 cm^{-1}. They derive, respectively, from the symmetric and asymmetric NH_2 stretching motions of the three formamide molecules linked separately to the NH_4^+ ion core via three $N-H^+\cdots O$ hydrogen bonds. Similarly distinct absorption features are also found for $H^+[HC(O)NH_2]_3$; moreover, they differ in frequency from the corresponding vibrational modes of $NH_4^+[HC(O)NH_2]_3$ by less than 10 cm^{-1}. The result is consistent with a picture of proton attachment to the oxygen atom, rather than the nitrogen atom in $H^+[HC(O)NH_2]_3$. We provide in this work both spectroscopic and computational evidence for the O-protonation of formamide and its clusters in the gas phase.

Introduction

Protonation is a fundamental process in organic and biological chemistry. It can be commonly found in acid-catalyzed addition and/or elimination reactions of carbonyl-containing compounds.[1] Studies of protonation are of importance from the viewpoint of biochemistry because it is the initial step involved in nonenzymatic hydrolysis of amides, peptides, and proteins in aqueous solutions.[2] Over the past few decades, investigations of these fundamentally important processes have mainly been limited to solution phases by using nuclear magnetic resonance (NMR) spectroscopy[3] in combination with isotope exchange techniques.[4] For the proton exchange between an amide [RC(O)NHR′] and the hydronium ion (H_3O^+), it has been a long scrutinized problem whether the protonation first occurs on the oxygen or on the nitrogen of RC(O)NHR′, as both atoms are capable of accepting the excess proton. Conceivably, the acid-catalyzed proton exchange can proceed either via the formation of a protonated imidic acid $RC(OH)=N^+HR'$ or via the formation of an N-protonated intermediate $RC(O)N^+H_2R'$ as

$$RC(O)N\mathit{H}R' + H^+ \leftrightarrow RC(OH)=N^+\mathit{H}R' \leftrightarrow RC(O)NHR' + \mathit{H}^+ \quad (1)$$

$$RC(O)N\mathit{H}R' + H^+ \leftrightarrow RC(O)N^+\mathit{H}HR' \leftrightarrow RC(O)NHR' + \mathit{H}^+ \quad (2)$$

Unfortunately, an unambiguous conclusion regarding whether route (1) or (2) is preferred for a given R/R′ is sometimes difficult to reach, even for the simplest amides in solution phases.[3] Experiments using charged water clusters as microsolvation matrices[5] to systematically study these reactions at varying stages of hydration are thus desired. Infrared spectroscopy, instead of NMR, can be used as the diagnostic tool for this analysis. We have recently successfully identified a number of isomeric structures of protonated ammonia−water clusters, $NH_4^+(H_2O)_n$,[6] protonated methylamine-water clusters, $CH_3NH_3^+(H_2O)_n$,[7] and other related species in a supersonic jet by employing vibrational predissociation spectroscopy and ab initio calculations. It is demonstrated therein that a combination of these two techniques is well suited for the detailed investigation of proton exchange and acid-catalyzed hydrolysis of amides in microsolvation water matrices.

Formamide (FA), the simplest molecule that contains one C(O)−N peptide bond and two functional groups (−C═O and $-NH_2$), serves as the prototype for this study. Being a prototypical system, formamide has been submitted to intensive investigations by ab initio calculations concerning its protonation,[8−15] dimerization,[16] ion−molecule association,[13,17,18] and acid/base-catalyzed hydrolysis.[8,19,20] The calculations accordingly predict that oxygen is the energetically more favored protonation site over the nitrogen by ∼15 kcal/mol. The prediction is in line with the amide resonance model,[21]

which enhances the basicity of the oxygen in this primary amide. Lin et al.[9] have attempted to verify the calculations by studying proton-transfer reactions between $D^+[HC(O)NH_2]$ and $HC(O)NH_2$ in a Fourier transform ion cyclotron resonance mass spectrometer, but obtained inconclusive results. It suggests a need of using spectroscopic methods to characterize the protonation site of formamide.

We present herein the first experimental evidence to support, although somewhat indirectly, the theoretical prediction that the oxygen has a higher proton affinity than the nitrogen in formamide. The evidence was obtained from a direct comparison of the vibrational spectra produced by calculation and measurement for the cluster ions $H^+[HC(O)NH_2]_3$ and $NH_4^+[HC(O)-$

[†] National Taiwan University.
[‡] Institute of Atomic and Molecular Sciences
[§] Present address: Institut für Angewandte Chemie Adlershof, D-12489 Berlin, Germany.

10.1021/jp000993n CCC: $19.00
Published on Web 09/30/2000

TABLE 1: Experimentally Observed and DFT-Calculated Stretching Frequencies (cm^{-1}) of Neutral and Protonated Formamide Monomers

expt.[a]	calc.[b]				assign-ments[d]
$HC(O)NH_2$(vapor)	$HC(O)NH_2$	**FA1I**[c]	**FA1II**[c]	**FA1III**[c]	
		3545	3502		νOH
3570	3571	3493	3481	3328	νNH
3448	3443	3379	3382	3321	νNH
				3226	νNH
2855	2875	3095	3126	3022	νCH
1755	1734	1720	1694	1867	νCO

[a] Reference 26. [b] Frequencies scaled by 0.963. [c] Structures illustrated in Figure 4. [d] See ref 26 for details.

$NH_2]_3$. A systematic comparison of the spectra between $H^+[HC(O)NH_2]_{1-3}$ and $NH_4^+[HC(O)NH_2]_{1-3}$ enabled us to establish a firm identification of the protonation site of formamide. In this paper, aside from providing experimental evidence for the O-protonation, the possibility of unconventional C−H···O bond formation between the formamide subunits in $H^+[HC(O)NH_2]_3$ is also addressed.

Methodologies

The methodologies employed in this work include both ab initio calculations[22] and vibrational predissociation spectroscopy.[6]

A. Calculations. Ab initio calculations were carried out using the commercial GAUSSIAN 94 program package.[23] Density functional theory (DFT) calculations, performed at the B3LYP/6-31+G* level of computation,[22,24] provide geometries, binding energies, vibrational frequencies, and infrared absorption intensities of various structural isomers to be compared with experimental measurements. In this calculation, geometries of the isomers were optimized by analytical gradients without imposing any symmetry constraints, and harmonic vibrational frequencies were obtained from analytical second derivatives. A vibrational frequency analysis served to identify the minima and/or transition states of the structures. Both basis set superposition errors and zero-point vibrational energies were corrected for the calculated total interaction energies.

For the clusters of interest in this work, we did not find any literature concerning the thermochemistry of the clustering,

$$H^+FA + (n-1)FA \rightarrow H^+(FA)_n \quad (3)$$

and

$$NH_4^+ + nFA \rightarrow NH_4^+(FA)_n \quad (4)$$

Hence, assessment of the accuracy of the calculations was made by comparing the calculated results to those of neutral formamide whose vibrational spectra have been well studied in the gas phase,[25−27] in Ar matrices,[26] and by previous ab initio calculations.[28] Table 1 compares the presently calculated frequencies with the observed vibrational modes of monomeric formamide in the gas phase. As noted, use of a single scaling factor (×0.963) successfully brings these two sets of data to close agreement for both the NH and CH stretches. The factor is thus used throughout this work.

B. Experiments. The experiments were conducted using a vibrational predissociation ion trap spectrometer combined with a pulsed infrared laser system. We generated protonated formamide with the aid of a corona discharge ion source by flowing $HC(O)NH_2$ vapor in pure H_2. The ion formed clusters with its neutral counterparts and other ingredients produced by the discharge in a supersonic expansion. Cluster ions with various sizes were first mass-selected by a 60° sector magnet and then spectroscopically analyzed by a tunable infrared laser inside an octopole ion trap. Upon excitation by resonant laser photons, the size-selected clusters dissociated predominantly via loss of a single formamide molecule. A quadrupole mass filter collected the photofragments, from which vibrational predissociation (action) spectra of the clusters were obtained.

Interesting proton-transfer reactions occurred during the corona-discharge supersonic expansion. A large number of $H^+[HC(O)NH_2]_nNH_3$ clusters were unexpectedly found, even when only $HC(O)NH_2/H_2$ was used as the gas sample mixture. The finding can be properly accounted for by the following reaction mechanism and energetics,

$$H_2 + e^- \rightarrow H_2^+ + 2e^- \quad (5)$$

$$H_2^+ + H_2 \rightarrow H_3^+ + H,\ \Delta H^\circ = -13.3\ \text{kcal/mol} \quad (6)$$

$$FA + H_3^+ \rightarrow (H^+FA)^* + H_2,\ \Delta H^\circ = -95.6\ \text{kcal/mol} \quad (7)$$

$$(H^+FA)^* \rightarrow NH_4^+ + CO,\ \Delta E_D = 69\ \text{kcal/mol} \quad (8)$$

It is noted that the energy release from reaction 7 is substantial, $\Delta H^\circ = -95.6$ kcal/mol, due to the large difference in proton affinity between H_2 and FA.[29] This generates internally hot species, denoted as $(H^+FA)^*$, which rapidly dissociates with a calculated dissociation barrier (ΔE_D) of 69 kcal/mol [eq 8].[9]

A tunable pulsed infrared laser was employed to prepare vibrationally excited formamide cluster ions at the frequency range of 2650−3850 cm^{-1} for CH, NH, and OH stretches. Unimolecular dissociation of this type

$$H^+(FA)_n \xrightarrow{h\nu} H^+(FA)_{n-1} + FA \quad (9)$$

or

$$H^+(FA)_3NH_3 \xrightarrow{h\nu} H^+(FA)_2NH_3 + FA \quad (10)$$

was induced by the excitation. While use of the infrared photons in this frequency range (2650−3850 cm^{-1}) supplies an energy of only 8−11 kcal/mol, which is typically lower than the dissociation energies of the cluster ions studied herein, fragmentation still can take place via two-photon absorption and/or via single-photon absorption at the expense of internal energies.[6,30] In this work, we determined the cluster temperature by measuring the spontaneous evaporation rate of the cluster of interest inside the octopole ion trap. With use of the DFT-calculated energies as the dissociation barriers (because no experimental data are yet available), fitting the measured evaporation rates to an evaporative ensemble model[31] allowed for an approximate estimation of the cluster temperature to be 170 K for both $H^+(FA)_3$ and $H^+(FA)_3NH_3$ investigated in this experiment. They contain an internal energy of roughly 3 kcal/mol, obtained from a simple statistical thermodynamics calculation.[6]

Results and Analysis

We classify the NH stretching modes of formamide according to how hydrogen bonding is made within the clusters. Resembling our previous classification of H_2O in water clusters,[32] the stretching modes of the $-NH_2$ group are characterized in terms

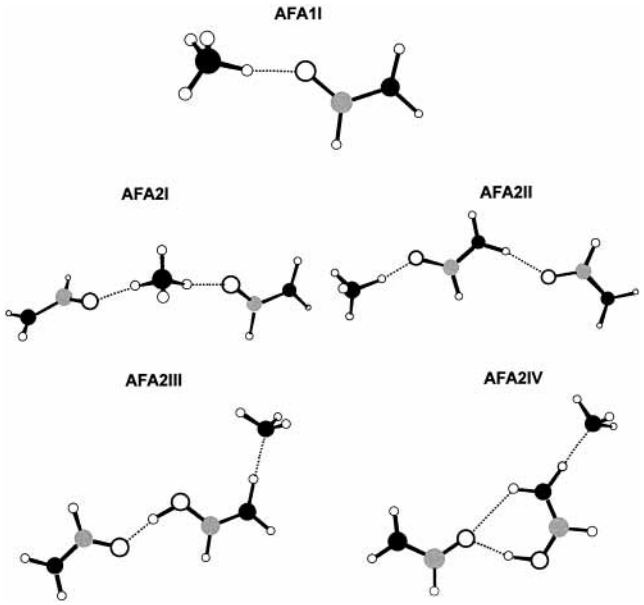

Figure 1. DFT-optimized structures of $H^+[HC(O)NH_2]NH_3$ and $H^+[HC(O)NH_2]_2NH_3$ isomers. The C, N, O and H atoms are denoted by shaded spheres, solid spheres, large open spheres, and small open spheres, respectively.

of asymmetric free-NH_2 (denoted as a-NH_2), symmetric free-NH_2 (denoted as s-NH_2), non-hydrogen-bonded free-NH (denoted as f-NH) and hydrogen-bonded-NH (denoted as b-NH) stretches. Note that, in formamide, there exists only one single amino group; whenever one of the two NH bonds is involved in hydrogen bonding, both the f-NH and b-NH stretches appear simultaneously. They constitute a pair, but distinctly different type, of transitions.

We began the investigation with $H^+[HC(O)NH_2]_nNH_3$, $n = 1-3$. The reason that this series of cluster ions was chosen to investigate is because ammonia has a proton affinity of 204.0 kcal/mol, higher than that of formamide by 7.5 kcal/mol;[29] hence, the isomers containing an NH_4^+ ion core with the formamide acting as a ligand molecule should dominate. It is expected from this experiment that one can obtain spectra that are easy to interpret and establish conclusive structural identification of isomers for these clusters. The result serves as a useful reference for latter identification of $H^+[HC(O)NH_2]_{1-3}$ isomers and, thereby, the energetically preferred protonation site of formamide.

A. $H^+[HC(O)NH_2]_nNH_3$. *A.1. n = 1 and 2.* Figure 1 depicts the lowest-energy structure of $H^+[HC(O)NH_2]NH_3$, denoted as **AFA1I**. Formation of this binary complex involves an ionic $N-H^+\cdots O$ hydrogen bond with the formamide aligned in a trans configuration (with respect to the C=O double bond of the formamide). In this hydrogen bond, the excess proton is located at a site closer to NH_3 than to FA, $d(N-H^+) = 1.081$ Å and $d(H^+\cdots O) = 1.559$ Å, yielding an NH_4^+ ion core.[33] The dominant source of the interaction is charge−dipole electrostatic forces between these two subunits. It is of interest to note that the calculated bond dissociation energy (ΔH_D) of this species is 28.8 kcal/mol (Table 2), which is substantially larger than that (24.8 kcal/mol)[34] between NH_4^+ and NH_3, even though FA has a lower proton affinity than NH_3 by 7.5 kcal/mol. This somewhat counterintuitive result is in close agreement with the finding of Meot-Ner[34] that the $N-H^+\cdots O$ hydrogen bond is in general stronger than $N-H^+\cdots N$ by 5.1 kcal/mol. We attribute the strong hydrogen bonding ($\Delta H_D = 28.8$ kcal/mol) between NH_4^+ and $HC(O)NH_2$ to the exceptionally large dipole moment (3.73 D)[35] of formamide due to its zwitterionic character.[21]

An attachment of the second FA molecule to isomer **AFAI** yields more than four stable isomers for $H^+(FA)_2NH_3$. Only trans isomers, which are ~1 kcal/mol more stable than their cis analogues, are discussed herein. Illustrated in Figure 1 is the optimized geometry of **AFA2I**, which contains an NH_4^+ ion sandwiched symmetrically between two FA ligand molecules. It is the lowest-energy isomer of $H^+(FA)_2NH_3$, as in the cases of $H^+(NH_3)_3$ (ref 36) and $H^+(H_2O)_2NH_3$.[6,7,22] The second-lowest energy isomer of this cluster is **AFA2II**, which consists of an FA dimer bound to NH_4^+ (Table 2). Interestingly, this binding results in a substantial elongation of the N^+-H bond pointing toward the FA molecule from $d(N-H^+) = 1.081$ Å of **AFA1I** to $d(N-H^+) = 1.115$ Å of **AFA2II**.[33] This effect of proton pulling, analogous to that of $H^+[(CH_3)_2O](H_2O)_n$ (ref 37) and $H^+(CH_3OH)(H_2O)_n$,[38] has been understood as a result of an enhancement in the proton affinity of FA due to dimerization. For $H^+(FA)_2NH_3$, it is possible that H^+FA-centered isomers also form when NH_3 is not in direct contact with the extra charge. The two representative isomers of this type are **AFA2III** and **AFA2IV**, both of which are less strongly bound than **AFA2I** by roughly 12 kcal/mol.

No vibrational predissociation spectrum was obtained for this dimer. The reasons that we failed to observe the spectrum of $H^+(FA)_2NH_3$ are believed to be two-fold. First, the energy required to rupture the ionic hydrogen bond of the lowest-lying isomer (**AFA2I**) is ~21 kcal/mol, which is much too high for the dissociation to occur upon one-photon or even two-photon excitation. Second, the relative abundance of the higher-energy isomers, such as **AFA2II** which has a higher probability to be dissociated by the infrared photons, is too low for us to observe their action spectra in the supersonic expansion.

TABLE 2: DFT-Calculated Stepwise and Total Energies (kcal/mol) of the Clustering via Channel (I) $NH_4^+ + n[HC(O)NH_2] \rightarrow H^+[HC(O)NH_2]_nNH_3$ or Channel (II) $H^+[HC(O)NH_2] + (n-1)[HC(O)NH_2] + NH_3 \rightarrow H^+[HC(O)NH_2]_nNH_3$

isomers[a]		B3LYP/6-31+G*			
$H^+[HC(O)NH_2]_{n-1}NH_3$	$H^+[HC(O)NH_2]_nNH_3$	ΔE_n(I)	ΔE_n(II)	$\Delta E_{n-1,n}$(I)	$\Delta E_{n-1,n}$(II)
	AFA1I	−28.8	−37.9		
AFA1I	**AFA2I**	−49.6	−58.7	−20.8	
AFA1I	**AFA2II**	−43.6	−52.7	−14.8	
AFA1I	**AFA2III**	−38.4	−47.6		−9.7
AFA1I	**AFA2IV**	−37.5	−46.6		−8.7
AFA2I	**AFA3I**	−65.6	−74.7	−16.0	
AFA2I	**AFA3II**	−65.4	−74.5	−15.8	
AFA2I	**AFA3III**	−59.8	−68.9	−10.2	
AFA2II	**AFA3IV**	−54.3	−63.4		−10.7
AFA2III	**AFA3V**	−53.4	−62.5		−14.9
AFA2III	**AFA3VI**	−53.2	−62.3		−14.7

[a] Structures illustrated in Figures 1 and 3.

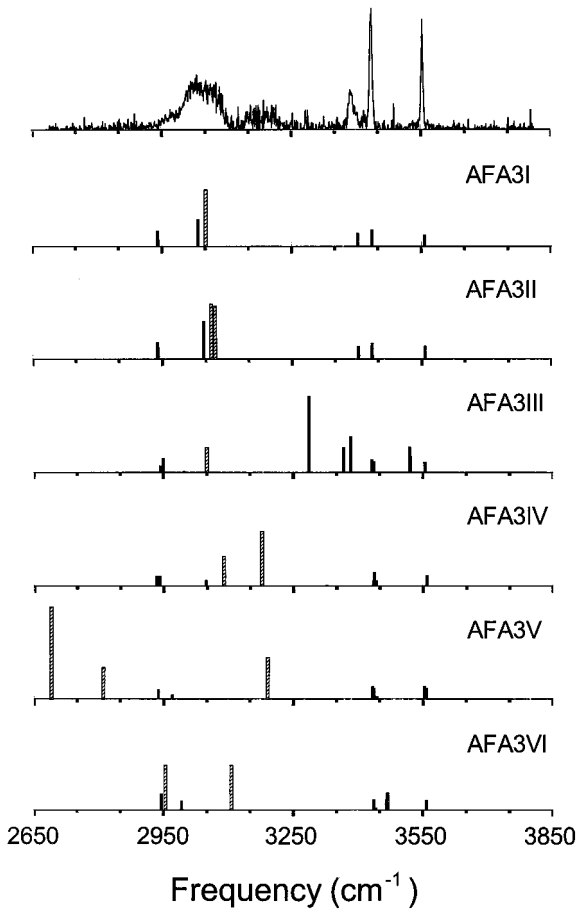

Figure 2. Comparison of the vibrational predissociation spectrum of $H^+[HC(O)NH_2]_3NH_3$ with the DFT-calculated stick diagrams of isomers depicted in Figure 3. The beam was expanded using a room-temperature nozzle and a typical stagnation pressure of 100 Torr. Formamide loss was monitored to obtain the experimental spectrum. Note that the calculated intensities of the free-NH and CH stretches (solid bars) have been amplified by a factor of 5 for clearer comparison to those of the bonded-NH stretches (slashed bars).

A.2. n = 3. Figure 2 compares the experimental spectrum of $H^+[HC(O)NH_2]_3NH_3$ to the DFT-calculated results. Two groups of transitions are discernible within the accessible frequency range of 2650−3850 cm^{-1}. They are the hydrogen-bonded-NH stretches of the NH_4^+ central ion at 2900−3100 cm^{-1} and the free-NH stretches of NH_4^+ and the $HC(O)NH_2$ ligand at 3300−3600 cm^{-1} (Table 3). Identification of the vibrational modes of NH_4^+ was made according to our previous studies of $NH_4^+(H_2O)_3$,[6] which has absorption bands located at 3375 cm^{-1} for the free-NH stretch and at 2962 and 3045 cm^{-1} for the bonded-NH stretches of the NH_4^+ ion core.

No indication was found for the f-NH stretching mode of formamide in the vicinity of 3500 cm^{-1} in the experimental spectrum. The lack of f-NH absorption bands in the spectrum supports the suggestion of an NH_4^+-centered structure, in which the three FA molecules are situated on the first solvation shell with their oxygen atoms attached to the NH_4^+ ion core in a linear $N-H^+\cdots O$ configuration.[6] There is only one type of FA in this cluster, as evidenced by the observation of the singlets at 3554 and 3436 cm^{-1} for a-NH_2 and s-NH_2, respectively. Such a suggestion of NH_4^+-centered structure is in accord with the theoretical prediction from DFT calculations that **AFA3I**, denoted as $NH_4^+(FA)_3$ in Figure 3, is the most stable structure out of the six geometrical isomers (Table 2). It is highly likely that the second-lowest energy isomer **AFA3II** is also responsible for the observed spectrum. This isomer, losing the C_3 symmetry, lies above **AFA3I** by only 0.2 kcal/mol. They both (**AFA3I** and **AFA3II**) are well separated in energy from the third NH_4^+-centered isomer (**AFA3III**) containing a second-shell FA, and are much more stable than isomers **AFA3IV**−**AFA3VI** consisting of an H^+FA ion core, as shown in Figure 3 and Table 2.

TABLE 3: Frequencies (cm^{-1}) and Assignments of the Observed NH Stretching Absorption Bands of $H^+[HC(O)NH_2]_3NH_3$

obsd freq	fwhm[a]	calcd freq[b]	isomers[c]	assignments
3554	5	3558, 3558, 3558	**AFA3I**	a-NH_2 of FA
		3558, 3558, 3558	**AFA3II**	a-NH_2 of FA
		3560, 3559	**AFA3IV**	a-NH_2 of FA
3436	6	3436, 3436, 3436	**AFA3I**	s-NH_2 of FA
		3436, 3436, 3436	**AFA3II**	s-NH_2 of FA
		3443, 3438	**AFA3IV**	s-NH_2 of FA
3422	9	3436, 3438, 3438	**AFA3IV**	free-NH of NH_3
3390	15	3402	**AFA3I**	free-NH of NH_4^+
		3404	**AFA3II**	free-NH of NH_4^+
3201	30	3178	**AFA3IV**	asym. b-NH of FA
3157	30	3089	**AFA3IV**	sym. b-NH of FA
3072	37	3071, 3063, 3045	**AFA3II**	bonded-NH of NH_4^+
3025	42	3051, 3050, 3033	**AFA3I**	bonded-NH of NH_4^+

[a] Full width at half-maximum. [b] Frequencies scaled by 0.963. [c] Structures illustrated in Figure 3.

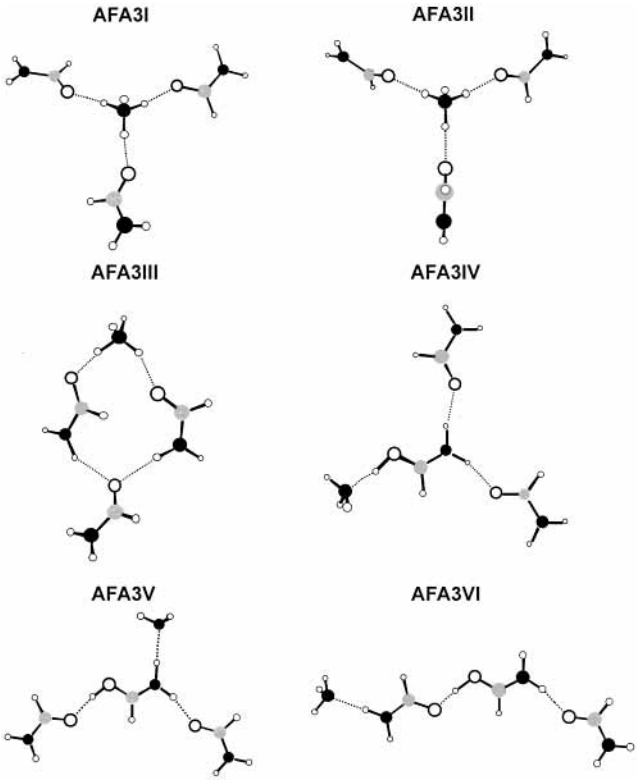

Figure 3. DFT-optimized structures of $H^+[HC(O)NH_2]_3NH_3$ isomers. The C, N, O and H atoms are denoted by shaded spheres, solid spheres, large open spheres, and small open spheres, respectively.

The simplicity of the experimental spectrum in Figure 2 allows for a near conclusive assignment of the 3390 cm^{-1} band to the free-NH stretching mode of NH_4^+ in **AFA3I** and **AFA3II**.[6] Given this assignment, one may associate the other two prominent features at ~3050 cm^{-1} with the bonded-NH stretches of NH_4^+, because their positions agree well with the corresponding band positions of $NH_4^+(H_2O)_3$ within 30 cm^{-1}.[6] A detailed assignment of these vibrational features to the NH_4^+-centered isomers is given in Table 3.

B. $H^+[HC(O)NH_2]_n$. *B.1. n = 1 and 2.* Figure 4 depicts the optimized structures of $H^+[HC(O)NH_2]$ from the B3LYP/6-

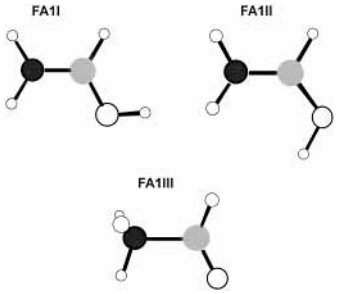

Figure 4. DFT-optimized structures of $H^+[HC(O)NH_2]$. The C, N, O and H atoms are denoted by shaded spheres, solid spheres, large open spheres, and small open spheres, respectively. The calculated protonation energies to attain the structures **FA1I**, **FA1II**, and **FA1III** are 193.1, 189.6, and 177.3 kcal/mol, respectively.

TABLE 4: DFT-Calculated Stepwise and Total Energies (kcal/mol) of the Clustering $H^+[HC(O)NH_2]$ + $(n-1)[HC(O)NH_2] \rightarrow H^+[HC(O)NH_2]_n$

isomers[a]		B3LYP/6-31+G*	
$H^+[HC(O)NH_2]_{n-1}$	$H^+[HC(O)NH_2]_n$	ΔE_n[b]	$\Delta E_{n-1,n}$
	FA1I	0.0	
	FA1II	3.5	
FA1I	**FA2I**	−34.3	−34.3
FA1I	**FA2II**	−31.2	−31.2
FA1I	**FA2III**	−29.7	−29.7
FA1I	**FA2IV**	−16.2	−16.2
FA2I	**FA3It**	−51.2	−16.9
FA2I	**FA3Ic**	−50.5	−16.2
FA2I	**FA3II**	−49.5	−15.2
FA2I	**FA3III**	−49.5	−15.2
FA2I	**FA3IV**	−46.6	−12.3
FA2I	**FA3V**	−45.5	−11.2
FA2I	**FA3VI**	−44.6	−10.3
FA2I	**FA3VII**	−45.0	−10.7

[a] Structures illustrated in Figs. 4, 5, and 8. [b] With respect to the total energy of isomer **FA1I**.

31+G* level of computation. Analogous to NH_4^+-FA, three isomers were found and they differ in protonation site and/or OH bond orientation with respect to the amino group. In agreement with prior predictions,[8−15] the O-protonation is much more favorable than the N-protonation by 15 kcal/mol (cf. the caption of Figure 4). Moreover, the O-protonated formamide **FA1I**, with the electron lone pair of the oxygen atom leaning toward the amino group, is significantly lower in energy than its conformer (**FA1II**) by 3.5 kcal/mol (cf. Table 4).

In Table 1, we compare the calculated frequencies (after scaling by ×0.963) of NH and CH stretches of isomers **FA1I**−**FA1III** to those of the neutral formamide. For **FA1I** (**FA1II**), both the a-NH_2 and s-NH_2 frequencies are predicted to be red-shifted by 78 (90) and 64 (61) cm^{-1}, respectively, due to the O-protonation. A much larger frequency red-shift (up to 300 cm^{-1}), however, was found for the NH stretches of isomer **FA1III**. These frequency red-shifts are so prominent that they can be used as a marker for the N-protonation.

Four DFT-optimized structures of $H^+[HC(O)NH_2]_2$ isomers are depicted in Figure 5, and they are all O-protonated. We neglect the N-protonated forms here because they lie much higher in energy and should have little contribution to our observations. Revealed by the DFT calculations, isomer **FA2I** is the global minimum with a binding energy of 34.3 kcal/mol (Table 4). In this binary complex, the two FA subunits are linked by a linear ionic O−H^+···O hydrogen bond with the two C−N peptide bonds aligned nearly anti-parallel to each other in a trans configuration. The corresponding cis configuration (**FA2II**) is less favorable, ∼3.1 kcal/mol higher in energy. The remaining

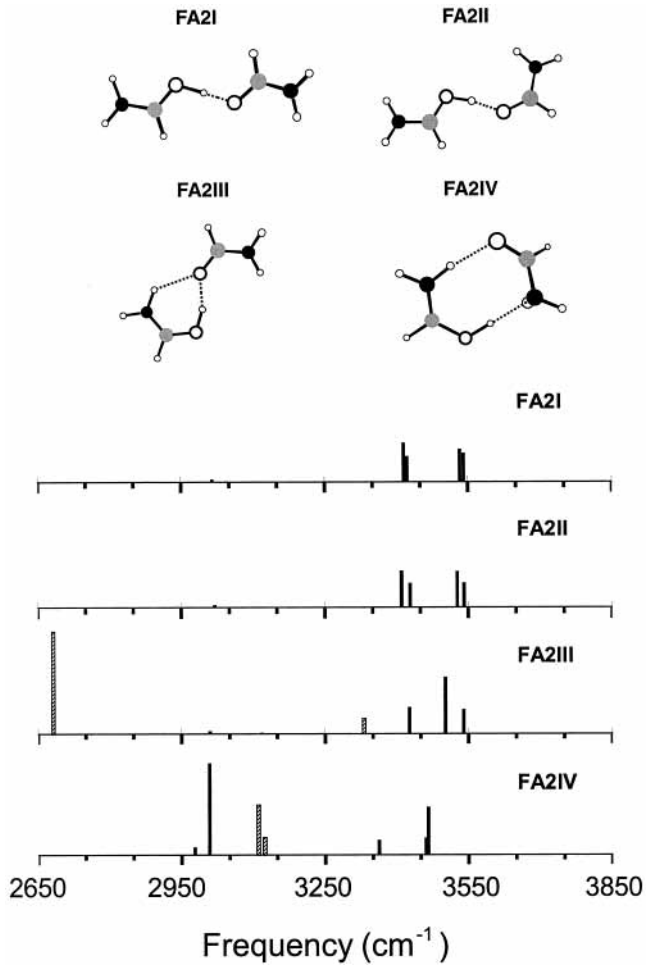

Figure 5. DFT-optimized structures of $H^+[HC(O)NH_2]_2$ isomers, where the C, N, O and H atoms are denoted by shaded spheres, solid spheres, large open spheres, and small open spheres, respectively. Shown underneath are the corresponding stick spectra of isomers **FA2I**−**FA2IV**. Note that the calculated intensities of the free-NH and CH stretches (solid bars) have been amplified by a factor of 5 for clearer comparison to those of the bonded-NH stretches (slashed bars).

two isomers (**FA2III** and **FA2IV**) contain multiple but nonlinear hydrogen bonds and are distinct in stability.

In this experiment, we were unable to obtain a good spectrum of $H^+(FA)_2$ for the same reasons as given for $H^+(FA)_2NH_3$ in the earlier section. In the absence of the experimental spectra, the calculated stick diagrams displayed in Figure 5 provide the most valuable insight into the observed spectra of the trimer discussed below.

B.2. n = 3. Figure 6 presents the vibrational predissociation spectrum of $H^+[HC(O)NH_2]_3$, showing two well-resolved a-NH_2 features at 3554 and 3545 cm^{-1} and three overlapping bands at 3446, 3436, and 3427 cm^{-1} for the s-NH_2 and f-NH stretches. Note that, the a-NH_2 bands are remarkably narrow, with a full width at half-maximum (fwhm) of only 4 cm^{-1} (cf. Figure 7a). They can be compared to the s-NH_2 stretches that have an fwhm of 7 cm^{-1} for each component of the barely resolved doublet at 3436 and 3427 cm^{-1}. Observation of such distinct band separations (∼9 cm^{-1}), which similarly appear in the spectra of isomers **FA2I** and **FA2II** (Figure 5) for both a-NH_2 and s-NH_2 stretches, indicates that there exist more than two distinct types of formamide in this cluster unit. We assign the lower-frequency pair (a-NH_2 and s-NH_2) of the two doublets to the formamide molecule in direct contact with the excess proton, and the higher-frequency pair (a-NH_2 and s-NH_2) of the doublets to the formamide molecule forming one N−H···O hydrogen

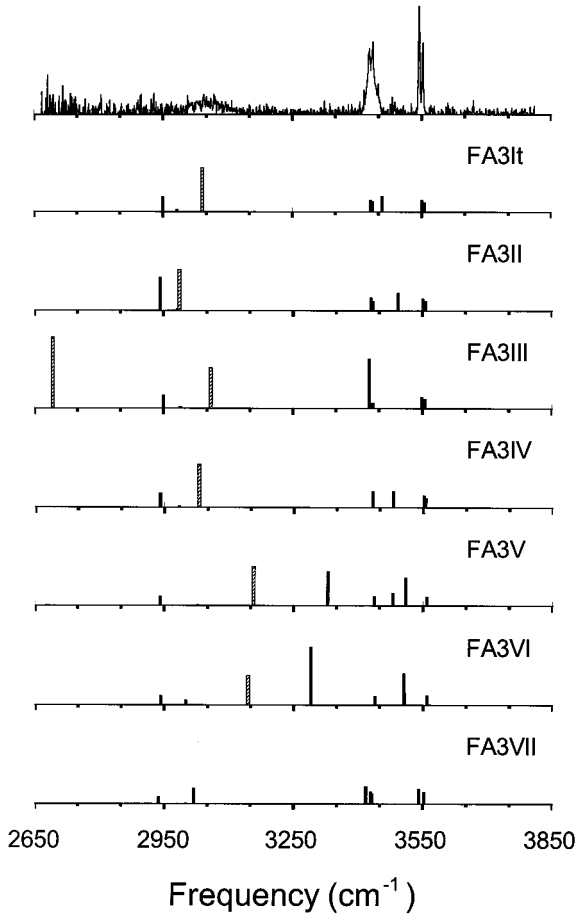

Figure 6. Comparison of the vibrational predissociation spectrum of $H^+[HC(O)NH_2]_3$ with the DFT-calculated stick diagrams of isomers depicted in Figure 5. The beam was expanded using a room-temperature nozzle and a typical stagnation pressure of 100 Torr. Formamide loss was monitored to obtain the experimental spectrum. Note that the calculated intensities of the free-NH and CH stretches (solid bars) have been amplified by a factor of 5 for clearer comparison to those of the bonded-NH stretches (slashed bars).

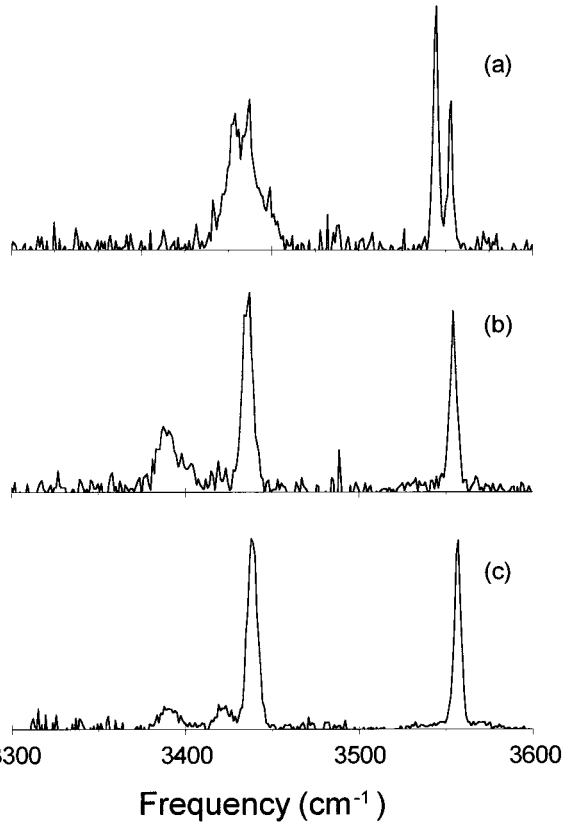

Figure 7. Enlarged views of the vibrational predissociation spectra of (a) $H^+[HC(O)NH_2]_3$, (b,c) $H^+[HC(O)NH_2]_3NH_3$ in the free-NH stretching region. Note that spectra (b) and (c) were obtained under different experimental conditions. A gas sample with saturated (unsaturated) vapor of liquid formamide seeded in H_2 was used to obtain the spectrum c (b). The two samples roughly differ 10-fold in formamide concentration.

bond with the amino group of the H^+FA ion core. The 3446 cm^{-1} band (fwhm = 9 cm^{-1}), obtained by Gaussian curve fitting, could then be associated with the f-NH stretch of the H^+FA whose b-NH stretching mode can accordingly be found as a broad absorption feature at 3046 cm^{-1} (cf. Figure 6).

We compare in Figure 6 the observed spectrum to the DFT-calculated stick diagrams of seven possible isomers **FA3It** and **FA3II**−**FA3VII**. The first isomer, denoted as **FA3It** in Figure 8, lies at the global minimum (cf. Table 4). It has a trans-trans arrangement with respect to the two C═O double bonds of the neutral formamide subunits, resulting in a stronger bonding than its trans-cis counterparts (**FA3Ic** and **FA3II**) by 1−2 kcal/mol and the cis−trans conformers (**FA3III** and **FA3IV**) by 2−4 kcal/mol. Compared to these linear isomers, **FA3V** and **FA3VI** are less strongly bound because they both contain an FA molecule situated on the second solvation shell of the H^+FA ion core. Note that among these eight isomers depicted in Figure 8, the linear noncyclic species (**FA3It**−**FA3II**) all contain a directional N−H···O hydrogen bond connecting the third FA molecule; hence, a dissociation energy of 16±1 kcal/mol is required to rupture the bond, yielding **FA2I** and monomeric FA as the final products. In contrast, a considerably lower energy (11±1 kcal/mol) is required for dissociation of the cyclic isomers **FA3V**−**FA3VII**. Of particular interest is isomer **FA3VII**, which contains an FA linked to the protonated dimer subunit by two unconventional C−H···O hydrogen bonds[39] with a total interaction energy of 10.7 kcal/mol (Table 4).

We emphasize that there are additionally more isomers than those presented here for the cluster $H^+(FA)_3$. They are mainly the cis analogues of the isomers depicted in Figure 8. Resembling that of **FA3It** and **FA3Ic**, the cis conformers of these isomers are all higher in energy than the corresponding trans forms by ∼1 kcal/mol. Also, the calculated spectra of the cis conformers are generally similar to those of the trans forms, except that the b-NH stretching frequencies of the former are significantly blue-shifted from the latter by ∼100 cm^{-1} because of weaker hydrogen bonding. These isomers are not discussed in detail herein to simplify the presentation of the analysis.

The features of the highest intensity in the experimental spectrum of $H^+(FA)_3$ (Figure 6) belong to a-NH_2 and s-NH_2 stretches. These stretches, notably, share close resemblance to the corresponding NH stretches in $NH_4^+(FA)_3$. Such a resemblance is particularly evident for the higher-frequency pair of the transitions, which agree in band position with those of the neutral formamide in $NH_4^+(FA)_3$ within 1 cm^{-1} (cf. Tables 3 and 5). For the lower-frequency pair of the transitions, they differ by only ∼10 cm^{-1}. Clearly, these frequency shifts are too small to be caused by a strong perturbation, such as the perturbation from protonation at the nitrogen site (cf. **FA1III** in Table 1). It suggests an attachment of the excess proton to the oxygen atoms, rather than to the nitrogen atoms, in this cluster. The good agreement reached by the close comparison of the observed spectrum with the calculated stick diagrams of **FA3It** in Figure 6 lends an experimental support to the theoretical calculations

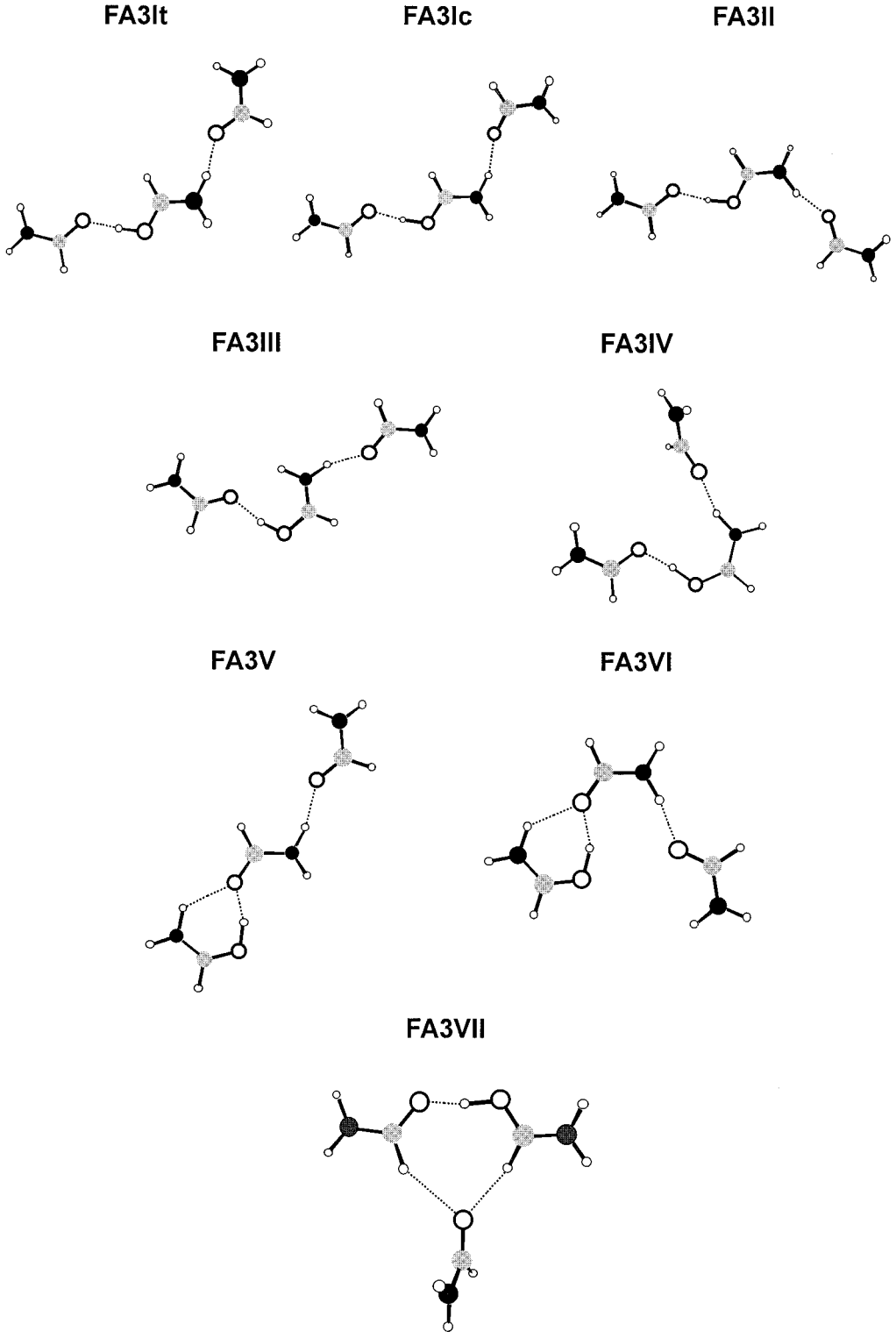

Figure 8. DFT-optimized structures of $H^+[HC(O)NH_2]_3$. The C, N, O and H atoms are denoted by shaded spheres, solid spheres, large open spheres, and small open spheres, respectively.

that the proton affinity of the oxygen is higher than that of the nitrogen in formamide.

Discussion

A. Identification of both H^+FA- and NH_4^+-Centered Isomers. Aside from **AFA3I** and **AFA3II**, an additional isomer can be identified from a close examination of the spectrum of $H^+[HC(O)NH_2]_3NH_3$ in Figure 2. The isomer (namely **AFA3IV**) is lowest in energy among the three H^+FA-centered forms, **AFA3IV**−**AFA3VI** (cf. Figure 3). In this isomer, the excess proton is located at a site closer to the formamide than to the ammonia [$d(O-H^+) = 1.063$ Å and $d(H^+\cdots N) = 1.542$ Å], despite that the NH_3 is in direct contact with this positive charge. The behavior, standing as an interesting contrast to that of **AFA1I** and **AFA2II** in Figure 1, is a direct consequence of the proton pulling effect discussed earlier.[37]

We identified the existence of isomer **AFA3IV** in the supersonic expansion from a simultaneous observation of the

TABLE 5: Frequencies (cm^{-1}) and Assignments of the Observed NH Stretching Absorption Bands of $H^+[HC(O)NH_2]_3$

obsd freq	fwhm[a]	calcd freq[b]	isomers[c]	assignments
3554	4	3556	FA3It	a-NH_2 of FA
3545	4	3551	FA3It	a-NH_2 of FA
3446[d]	9	3458	FA3It	f-NH of H^+FA
3436[d]	7	3436	FA3It	s-NH_2 of FA
3427[d]	7	3431	FA3It	s-NH_2 of FA
3046	100	3075	FA3It	b-NH of H^+FA

[a] Full width at half-maximum. [b] Frequencies scaled by 0.963. [c] Structures illustrated in Figure 8. [d] Obtained by band deconvolution.

weak but reproducible feature at 3422 cm^{-1} (Figures 7b and 7c) and the well-resolved doublet at 3157 and 3201 cm^{-1} (Figure 2). For the former, the band position is close to that of the free-NH stretches (at 3417 cm^{-1}) of the neutral NH_3 in $NH_4^+(NH_3)_n$ (ref 36) and, therefore, it can be assigned to the same stretch of NH_3 acting as a proton-accepting ligand of H^+FA in $H^+(FA)_3$-NH_3. The latter can be associated with the symmetric and asymmetric bonded-NH stretches of the H^+FA ion core, whose NH_2 bonds are both involved in hydrogen bonding as in liquid formamide.[40] These bonded-NH vibrations are noticeably higher in frequency than the corresponding b-NH stretch of $H^+(FA)_3$ at 3046 cm^{-1} due to hydrogen bond anti-cooperative effects.[22]

Figures 7b and 7c compare the spectra of $H^+(FA)_3NH_3$ synthesized under different experimental conditions to further emphasize the coexistence of H^+FA-centered and NH_4^+-centered isomers in the supersonic expansion.[41] As clearly seen from the figure, the intensity ratio of the bands at 3390 and 3422 cm^{-1}, which are the fingerprints of these two distinct types of isomers, can vary sensitively with the gas composition. An equality in intensity was obtained when saturated formamide vapor seeded in H_2 was used as the gas sample for the corona-discharged supersonic expansion.

A questions may be raised: How can the H^+FA-centered isomers be observed by the present experiment since they lie so much higher in energy than the corresponding NH_4^+-centered isomers? We believe that the answer is closely associated with the clustering kinetics involved in the supersonic expansion, the dynamics of interconversion between NH_4^+- and H^+FA-centered forms, and the difference in excitation scheme between these two types of isomers. In this work, the clusters of interest are produced by an adiabatic expansion, which is a nonequilibrium process. Hence, clustering kinetics, in addition to energetics, should govern the relative abundance of the cluster isomers in the beam. One may expect that when the $H^+(FA)_3$-NH_3 ions are produced adiabatically, statistically some of them should be centered with H^+FA. These H^+FA-centered isomers can be easily trapped in this configuration because, in order to have them converted to the corresponding NH_4^+-centered isomers, a high barrier must be overcome. It involves a large movement of the FA molecule from one side of the H^+FA ion core to another, which is clearly not an energetically favorable process.

Previously,[6] we demonstrated in the study of $NH_4^+(H_2O)_{3-6}$ that the vibrational predissociation involved therein is primarily a one-photon process. Such a process prevails because the energies required to dissociate these cluster ions are relatively low, ranging from 10 to 13 kcal/mol, and the dissociation can occur at the expense of required internal energies. For the present dissociation of **AFA3I** and **AFA3II**, however, more than one photon should be needed because these isomers are all bound with a dissociation energy of ~16 kcal/mol (Table 2). Shown in Figure 9 is the experimental measurement on the dependence

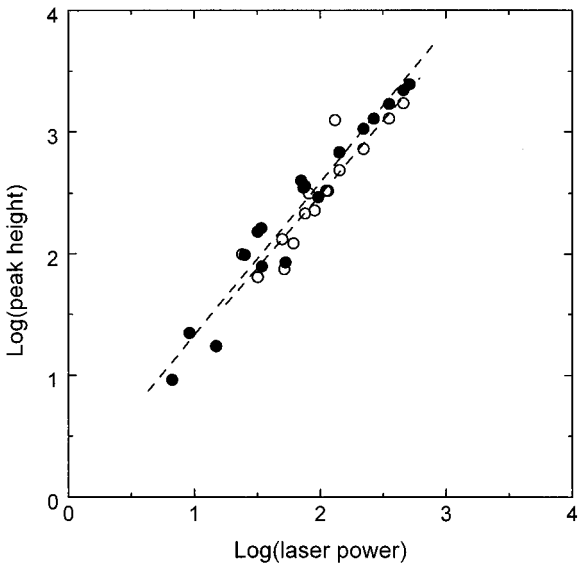

Figure 9. Dependence of fragment ion intensity on laser power density for *a*-NH_2 (●) and s-NH_2 (○) stretches of $H^+[HC(O)NH_2]_3NH_3$. Dashed lines are the best fits of the experimental data to the nonlinear power law, (peak height) ∝ (laser power)^n. An average of $n = 1.3$ photons/excitation is required for the dissociation of $H^+[HC(O)NH_2]_3NH_3$ for both NH stretches.

of the peak intensities of a-NH_2 and s-NH_2 absorption bands on laser pulse energy for $H^+[HC(O)NH_2]_3NH_3$. Within the energy range used in this experiment, the power dependence is clearly nonlinear. A statistical average of 1.3 photons per excitation is required for the dissociation of these clusters, indicating that a significant portion of the observed signal is derived from a two-photon process. It should be noted that while the H^+FA-centered cluster isomer **AFA3IV** may exist in a substantially less amount than **AFA3I** and **AFA3II** in the beam due to weaker hydrogen bonding, it can be detected more easily by this vibrational predissociation ion trap spectrometer via one-photon excitation process.

B. Implications for C−H···O Formation. Comparison of the spectra in Figure 6 favors an assignment of the observed vibrational features to isomer **FA3It** rather than to **FA3II**−**FA3VI** (Table 5). We notice, however, that the b-NH absorption band as observed experimentally is significantly lower in intensity than that predicted for **FA3It**. It seems to suggest the presence of a second isomer. A close inspection of the eight structures (and their cis conformers) depicted in Figure 8 reveals that isomer **FA3VII** is the only species without a b-NH group. The other seven isomers all contain one pair of transitions, belonging to f-NH and b-NH stretches, in their calculated spectra. Hence, according to the present calculations, the fact that we failed to observe an intense b-NH absorption band in the experimental spectrum (Figure 6) implies that isomer **FA3VII**, while not lowest in energy, might make a significant contribution to the observation. We have attempted a temperature dependence measurement[30] to verify the presence of this isomer but, unsuccessfully, the temperature range we could vary is too small to allow us to observe any significant changes in the spectrum. It remains a challenge to establish a conclusive identification of this intriguing species in the supersonic expansion.

The prediction for the existence of isomer **FA3VII** in Table 4 ties in to our previous identification of the unconventional C−H···O bond formation in $[(CH_3)_2O]_2H^+-H_2O$.[30] It also links this work with the studies of C−H···O hydrogen bonds[42] in biomolecular crystals. In a series of studies of C−H···O contacts

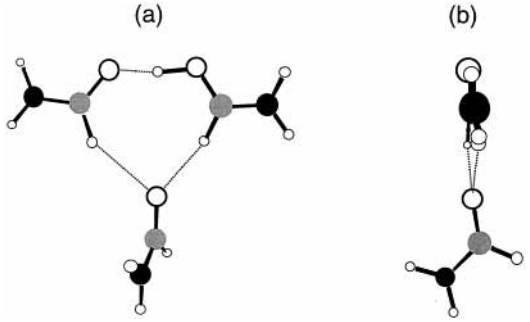

Figure 10. (a) Front view and (b) side view of the H^+FA-centered **FA3VII** structure. The C, N, O and H atoms are denoted by shaded spheres, solid spheres, large open spheres, and small open spheres, respectively.

using neutron scattering, Steiner[43] found a good correlation between the covalent $C_\alpha-H$ bond length and the $H_\alpha\cdots O$ separation in 16 zwitterionic compounds and chloride salts of α-amino acids. For the shortest contact with an $H_\alpha\cdots O$ separation of ~2.3 Å, the associated $C_\alpha-H$ bond is lengthened by up to 0.008 Å. Evidence for the existence of an ionic C−H to O hydrogen bond in large biomolecules has also been provided by Musah et al.[44] using cationic heterocyclic compounds as the guest molecules in an engineered protein cavity. They obtained an energy of ~15 kcal/mol, contributed mostly from electrostatic forces, for the binding of a thiazole cation to the aspartic acid of the cytochrome *c* peroxidase.

Figure 10 presents the front view and side view of the **FA3VII** structure. It consists of two unconventional C−H···O bonds and three FA units lying in two nearly perpendicular planes. The bond lengths and angles of these two C−H···O contacts substantially differ, with $d(H\cdots O) = 2.05/2.34$ Å and $\angle C-H\cdots O = 163°/148°$. The former ($d = 2.05$ Å) is clearly much shorter than the corresponding bond length of ~2.3 Å in molecular crystals of α-amino acids.[43] Note that in this structure (Figure 10), the two electron lone pairs of the oxygen atom lie in a plane tilted ~5° from the normal to the plane containing the two C−H bonds; hence, the overlap of molecular orbitals between these hydrogen-bonded O and H atoms is minimal. Such unconventional C−H···O bonding, with the O═C−N dipole pointing directly toward the excess proton, is purely electrostatic, mainly through charge−dipole interactions.

Conclusions

We have collected and assigned the infrared spectra of formamide-containing cluster cations synthesized by a supersonic expansion. The clusters display characteristic absorption features derived from the asymmetric and symmetric free-NH_2 stretches of $HC(O)NH_2$ hydrogen-bonded to either the $HC(OH)=N^+H_2$ or the NH_4^+ ion core. Despite a large number of calculations having been performed before us to predict the protonation site of formamide, we provide the first spectroscopic data to compare with theory. From a detailed analysis of the spectra of $H^+[HC(O)NH_2]_3$ and $NH_4^+[HC(O)NH_2]_3$, it is concluded that infrared spectroscopy can be used as a tool to characterize the protonation property of this primary amide. The method is capable of delineating the protonation properties of higher-order amides, or even polypeptides.

Results of this work suggest an interesting possibility of C−H···O bond formation in the protonated formamide trimer, $H^+[HC(O)NH_2]_3$, where the three amide groups are bridged by two ionic C−H···O hydrogen bonds. The study of these unconventional hydrogen bonds may provide useful insight into the C−H···O interactions in biomolecules, particularly in proteins or polypeptides. Whether these types of interactions can actually exist in biomolecules and how they affect the protein folding processes[45] is an interesting subject to address in future experiments.

Acknowledgment. We thank the Academia Sinica and the National Science Council (Grant No. NSC 89-2113-M-001-036-CT) of Taiwan, the Republic of China, for financial support.

Supporting Information Available: Files containing the supplementary information are described in reference 33. These files can be opened with the program Chem 3-D to retrieve the geometry information. This material is available free of charge via the Internet at http://pubs.acs.org.

References and Notes

(1) Lowry, T. H.; Richardson, K. S. *Mechanism and Theory in Organic Chemistry*; 3rd ed.; Harper & Row: New York, 1987.
(2) Hill, R. L. In *Advances in Protein Chemistry*; Anfinsen, C. B., Anson, M. L., Edsall, J. T., Richards, F. M., Eds.; Academic Press: New York, 1965; p 37.
(3) Perrin, C. L. *Acc. Chem. Res.* **1989**, *22*, 268.
(4) Brown, R. S.; Bennet, A. J.; Slebocka-Tilk, H. *Acc. Chem. Res.* **1992**, *25*, 481.
(5) Achatz, U.; Joos, S.; Berg, C.; Schindler, T.; Beyer, M.; Albert, G.; Niedner-Schatteburg, G.; Bondybey, V. E. *J. Am. Chem. Soc.* **1998**, *120*, 1876.
(6) Wang, Y.-S.; Chang, H.-C.; Jiang, J. C.; Lin, S. H.; Lee, Y. T.; Chang, H.-C. *J. Am. Chem. Soc.* **1998**, *120*, 8777.
(7) Chang, H.-C.; Wang, Y.-S.; Lee, Y. T.; Chang, H.-C. *Int. J. Mass Spectrom.* **1998**, *180*, 91.
(8) Laidig, K. E.; Bader, R. F. W. *J. Am. Chem. Soc.* **1991**, *113*, 6312. Krug, J. P.; Popelier, P. L. A.; Bader, R. F. W. *J. Phys. Chem.* **1992**, *96*, 7604.
(9) Lin, H.-Y.; Ridge, D. P.; Uggerud, E.; Vulpius, T. *J. Am. Chem. Soc.* **1994**, *116*, 2996.
(10) Antoczak, S.; Ruiz-Lopez, M. F.; Rivail, J. L. *J. Am. Chem. Soc.* **1994**, *116*, 3912.
(11) Casteiger, J.; Hondelmann, U.; Rose, P.; Witzenbichler, W. *J. Chem. Soc., Perkin Trans. 2*, **1995**, 193.
(12) Ou, M.-C.; Chu, S.-Y. *J. Phys. Chem.* **1995**, *99*, 556.
(13) Tortajada, J.; Leon, E.; Morizur, J.-P.; Luna, A.; Mó, O.; Yáñez, M. *J. Phys. Chem.* **1995**, *99*, 13890.
(14) Pranata, J.; Davis, G. D. *J. Phys. Chem.* **1995**, *99*, 14340. Kamitakahara, A.; Pranata, J. *J. Mol. Struct.* **1998**, *429*, 61.
(15) Cho, S. J.; Cui, C.; Lee, J. Y.; Park, J. K.; Suh, S. B.; Park, J.; Kim, B. H.; Kim, K. S. *J. Org. Chem.* **1997**, *62*, 4068.
(16) Colominas, C.; Luque, F. J.; Orozco, M. *J. Phys. Chem. A* **1999**, *103*, 6200.
(17) Luna, A.; Amekraz, B.; Tortajada, J.; Morizur, J.-P.; Alcamí, M.; Mó, O.; Yánñz, M. *J. Am. Chem. Soc.* **1998**, *120*, 5411.
(18) Cabaleiro-Lago, E. M.; Rios, M. A. *J. Chem. Phys.* **1999**, *110*, 6782.
(19) Marlier, J. F.; Dopke, N. C.; Johnstone, K. R.; Wirdzig, T. J. *J. Am. Chem. Soc.* **1999**, *121*, 4356.
(20) Bakowies, D.; Kollman, P. A. *J. Am. Chem. Soc.* **1999**, *121*, 5712.
(21) Fogarasi, G.; Szalay, P. G. *J. Phys. Chem. A* **1997**, *101*, 1400.
(22) Jiang, J. C.; Chang, H.-C.; Lee, Y. T.; Lin, S. H. *J. Phys. Chem. A* **1999**, *103*, 3123.
(23) Frisch, M. J.; Trucks, G. W.; Schlegel, H. B.; Gill, P. M. W.; Johnson, B. G.; Robb, M. A.; Cheeseman, J. R.; Keith, T.; Petersson, G. A.; Montgomery, J. A.; Raghavachari, K.; Al-Laham, M. A.; Zakrzewski, V. G.; Ortiz, J. V.; Foresman, J. B.; Cioslowski, J.; Stefanov, B. B.; Nanayakkara, A.; Challacombe, M.; Peng, C. Y.; Ayala, P. Y.; Chen, W.; Wong, M. W.; Andres, J. L.; Replogle, E. S.; Gomperts, R.; Martin, R. L.; Fox, D. J.; Binkley, J. S.; Defrees, D. J.; Baker, J.; Stewart, J. P.; Head-Gordon, M.; Gonzalez, C.; Pople, J. A. *Gaussian 94*, Revision D.3, Gaussian, Inc.: Pittsburgh, PA, 1995.
(24) Gruenloh, C. J.; Carney, J. R.; Arrington, C. A.; Zwier, T. S.; Fredericks, S. Y.; Jordan, K. D. *Science* **1997**, *276*, 1678.
(25) Evans, J. C. *J. Chem. Phys.* **1959**, *31*, 1435.
(26) King, S. T. *J. Phys. Chem.* **1971**, *75*, 405.
(27) Brummel, C. L.; Shen, M.; Hewett, K. B.; Philips, L. A. *J. Opt. Soc. Am. B* **1994**, *11*, 176.
(28) Kwiatkowski, J. S.; Leszczynski, J. *J. Mol. Struct.* **1993**, *297*, 277.
(29) Hunter, E. P. L.; Lias, S. G. *J. Phys. Chem. Ref. Data* **1998**, *27*, 413.

(30) Hahndorf, I.; Jiang, J. C.; Chang, H.-C.; Wu, C.-C.; Chang, H.-C. *J. Phys. Chem. A* **1999**, *103*, 8753.

(31) Klots, C. E. *Z. Phys. D.* **1991**, *20*, 105.

(32) Jiang, J. C.; Chang, J.-C.; Wang, B.-C.; Lin, S. H.; Lee, Y. T.; Chang, H.-C. *Chem. Phys. Lett.* **1998**, *289*, 373.

(33) Detailed information on the bond angles, lengths and the proton pulling effects is available on the World Wide Web at http://po.iams.sinica.edu.tw/lab/hcchang/wcche/index.html.

(34) Meot-Ner, M. *J. Am. Chem. Soc.* **1984**, *106*, 1257.

(35) Lide, D. R., Ed. *CRC Handbook of Chemistry and Physics*; 75th ed.; CRC Press: Boca Raton, 1994.

(36) Price, J. M.; Crofton, M. W.; Lee, Y. T. *J. Chem. Phys.* **1989**, *91*, 2749; *J. Phys. Chem.* **1991**, *95*, 2182.

(37) Chang, H.-C.; Jiang, J. C.; Hahndorf, I.; Lin, S. H.; Lee, Y. T.; Chang, H.-C. *J. Am. Chem. Soc.* **1999**, *121*, 4443.

(38) Wu, C.-C.; Jiang, J. C.; Boo, D. W.; Lin, S. H.; Lee, Y. T.; Chang, H.-C. *J. Chem. Phys.* **2000**, *112*, 176

(39) Meot-Ner, M.; Deakyne, C. A. *J. Am. Chem. Soc.* **1985**, *107*, 469.

(40) Suzuki, I. *Bull. Chem. Soc. Jpn.* **1960**, *33*, 1359.

(41) The coexistence of both NH_4^+ and H^+FA ion cores in $H^+(FA)_3NH_3$ is similar to that of H_3O^+ and $CH_3OH_2^+$ simultaneously observed for the mixed methanol water clusters (ref 38 and Chaudhuri, C.; Jiang, J. C.; Wang, X.; Lee, Y. T.; Chang, H.-C. *J. Chem. Phys.* **2000**, *112*, 7279).

(42) Gu, Y.; Kar, T.; Scheiner, S. *J. Am. Chem. Soc.* **1999**, *121*, 9411, and references therein.

(43) Steiner, T. *J. Chem. Soc., Perkin Trans. 2* **1995**, 1315.

(44) Musah, R. A.; Jensen, G. M.; Rosenfeld, R. J.; McRee, D. E.; Goodin, D. B. *J. Am. Chem. Soc.* **1997**, *119*, 9083.

(45) See the special issue of *Acc. Chem. Res.* **1998**, *31*, 1.